International Journal of Architectural, Civil and Construction Sciences
ISSN: 2415-1734
Vol:13, No:9, 2019

First Cracking Moments of Hybrid Fiber Reinforced Polymer-Steel Reinforced Concrete Beams

Saruhan Kartal, Ilker Kalkan

***Abstract*—**The present paper reports the cracking moment estimates of a set of steel-reinforced, Fiber Reinforced Polymer (FRP)-reinforced and hybrid steel-FRP reinforced concrete beams, calculated from different analytical formulations in the codes, together with the experimental cracking load values. A total of three steel-reinforced, four FRP-reinforced, 12 hybrid FRP-steel over-reinforced and five hybrid FRP-steel under-reinforced concrete beam tests were analyzed within the scope of the study. Glass FRP (GFRP) and Basalt FRP (BFRP) bars were used in the beams as FRP bars. In under-reinforced hybrid beams, rupture of the FRP bars preceded crushing of concrete, while concrete crushing preceded FRP rupture in over-reinforced beams. In both types, steel yielding took place long before the FRP rupture and concrete crushing. The cracking moment mainly depends on two quantities, namely the moment of inertia of the section at the initiation of cracking and the flexural tensile strength of concrete, i.e. the modulus of rupture. In the present study, two different definitions of uncracked moment of inertia, i.e. the gross and the uncracked transformed moments of inertia, were adopted. Two analytical equations for the modulus of rupture (ACI 318M and Eurocode 2) were utilized in the calculations as well as the experimental tensile strength of concrete from prismatic specimen tests. The ACI 318M modulus of rupture expression produced cracking moment estimates closer to the experimental cracking moments of FRP-reinforced and hybrid FRP-steel reinforced concrete beams when used in combination with the uncracked transformed moment of inertia, yet the Eurocode 2 modulus of rupture expression gave more accurate cracking moment estimates in steel-reinforced concrete beams. All of the analytical definitions produced analytical values considerably different from the experimental cracking load values of the solely FRP-reinforced concrete beam specimens.

***Keywords*—**Cracking moment, four-point bending, hybrid use of reinforcement, polymer reinforcement.

I. Introduction

DURABILITY problems associated with the corrosion of steel are quite common in conventional reinforced concrete (RC) members. FRP bars constitute an efficient alternative to steel reinforcement due to their high corrosion resistance and high tensile strength. However, FRP bars also have some significant disadvantages, including sudden and brittle failure, low modulus of elasticity, non-ductile behavior. Different types of FRP bars (CFRP-Carbon Fiber Reinforced Polymer, GFRP, BFRP, AFRP- Aramid Fiber Reinforced Polymer, VFRP-Vinyl Fiber Reinforced Polymer) were used in the previous studies as reinforcement for concrete, which reported that concrete beams reinforced with FRP bars do not exhibit adequate ductility compared to steel-RC beams. In addition, due to their low modulus of elasticity as compared to steel reinforcement, considerable deflections and crack widths are encountered in FRP-RC beams under service conditions.

The idea of using FRP bars together with steel bars in the tension zone of a concrete beam, i.e. the hybrid use of FRP and steel bars, was offered as an effective reinforcement scheme to encounter all of the aforementioned disadvantages of the sole use of FRP and steel. The contribution of steel reinforcement to hybrid RC beams originates from the ductility and high modulus of elasticity of this material, while the contribution of FRP bars stems from the high tensile strength and high corrosion resistance. Thus, hybrid-RC beams show adequate ductility and service performance.

The authors are aware of a very limited number of studies on the flexural behavior of hybrid-RC beams in the literature. Some of these studies are presented herein. Aiello and Ombres [1] studied deflection, curvature, ductility and cracking behavior of hybrid AFRP-steel RC beams, focusing on their ultimate and service limit states. Leung and Balendran [2] investigated the effects of concrete compressive strength and hybrid reinforcement ratio on the bending behavior of hybrid GFRP-steel RC beams. Qu [3] investigated the effects of reinforcement amount and GFRP/steel ratio on the bending behavior of hybrid GFRP-steel RC beams. The simultaneous use of the steel and GFRP bars was shown to improve the bending behavior of the beam as compared to the sole use of GFRP reinforcing bars. Lau and Pam [4] investigated the bending behavior of pure GFRP, pure steel and hybrid GFRP-steel RC beams. In their study, bending strength and ductility were adopted as the main parameters. Safan [5] investigated the failure modes, cracking and load deflection behavior of hybrid GFRP-steel RC beams. In the study conducted by Yinghao and Yong [6], the bending capacity, beam stiffness and cracking of hybrid GFRP-steel RC beams with high concrete strength was investigated. Yaz [7] studied flexural behavior of hybrid GFRP-steel RC beams. Increasing the steel reinforcement ratio was established to result in a more ductile behavior, whereas decreasing the deformability of the beam corresponding to maximum load.

The aforementioned studies in the literature focused on the flexural behavior, failure modes, load-carrying capacities, deformations and cracking of hybrid-RC beams. There are no studies, known to the authors, related to the first cracking moment estimates of these beams. In the present study, the initial cracking moment values of the hybrid FRP-steel over- and under-RC beams were estimated using the modulus of rupture formulations of different structural concrete codes [8], [9] together with different uncracked moment of inertia

Saruhan Kartal and Ilker Kalkan are with the Department of Civil Engineering, Faculty of Engineering, Kirikkale University, 71450 Kirikkale, Turkey (e-mail: saruhankartal@kku.edu.tr, ilkerkalkan@kku.edu.tr).

expressions and compared to the experimental cracking moment values. The expressions yielding to the closest estimates in steel-reinforced, FRP-reinforced and hybrid over- and under-reinforced beam groups were established.

II. Experimental Study

A. Specimens

In the present study, two types of FRP bars, namely GFRP and BFRP bars, were used. Within this scope, a total of 24 half-scale concrete beam specimens, including three steel-reinforced, four FRP-reinforced and 17 hybrid steel-FRP reinforced, were tested under four-point bending (two-point loading). The capital letters in the specimen notations indicate the type of rebars used in the specimen. B, G and S stand for BFRP, GFRP and steel tension reinforcing bars, respectively. The number after each letter shows the number of that type of bar in the tension zone.

The test matrix was composed of four groups based on the type of reinforcing bar and failure mode. The first group was made up of the reference specimens S3, S5 and S6, which have three, five and six steel tension rebars, respectively. In the second group, the reference specimen B5 with five BFRP bars and the reference specimens G3, G5 and G6 with three, five and six GFRP bars, respectively, were tested. The third group was composed of a total of 12 hybrid over-RC beams, reinforced with BFRP-steel or GFRP-steel bars. The final group, on the other hand, was composed of five hybrid under-RC beams with BFRP-steel or GFRP-steel reinforcing bars (Table I).

B. Material Properties

The steel tension bars (ϕ12) in the beams were of grade 420 and their tensile strength was determined as 470 MPa from the material tests. In the present study, one type of BFRP and two types of GFRP reinforcement were used. The mechanical properties of the materials are shown in Table I together with the other details of the specimens. The specimens of the present study were cast in two separate batches. The compressive and tensile strength values of each beam were determined from the material tests on concrete cylinders and prisms, taken during each cast. The average concrete strength values were measured as 31.28 and 30.49 MPa for the two batches and the respective flexural tensile strength values as 3.55 and 3.25 MPa.

C. Test Specimens and Setup

The cross-sectional dimensions of the beams are given in Table I. Each beam had a total length of 3000 mm and a clear span length of 2800 mm. With the exception of the central constant moment region of the beam, each beam (shear spans) was reinforced with two-legged ϕ8 stirrups with a spacing of 100 mm. Moreover, no compression reinforcement was used in the central maximum moment (zero-shear) region of the beams, cast in the second batch, while the beams of the first batch contained 2 Ø10 steel compression bars along the whole beam length. This is indicated in Fig. 1, which also illustrates the test setup.

The beams were tested under two-point loading and simple support conditions at the ends. The vertical deflections were measured at the front and rear faces of the beam at mid-span in order to eliminate any possible effect of torsion on the deflection measurements and to eliminate the risk of the inadequacy of the stroke of LVDT's. The test setup is depicted in Fig. 1 in detail.

III. Analytical Calculations

The main aim of the present study is to estimate the cracking moments of RC beams with only steel, only FRP and hybrid FRP-steel reinforcement analytically and evaluate the accuracy of the analytical estimates by comparing them to the experimental cracking moment values. The cracking moment depends fundamentally on two parameters, namely the moment of inertia of the section at the initiation of cracking and the tensile strength of concrete at this level. The moment of inertia represents the resistance of the section to bending moments, while the flexural tensile strength (modulus of rupture) reflects the material strength against bending. In the present section, first different moment of inertia expressions that can be used in analytical calculations are presented. In the second part of this section, on the other hand, different modulus of rupture expressions are presented.

A. Moment of Inertia Definitions

There are two different definitions of moment of inertia that can be used for calculating the first cracking moments of *RC* beams. The first one of these definitions is the gross moment of inertia (I_g), which is based on the assumption that the whole cross-section behaves as a single solid body at the uncracked stage of the flexural behavior and neglects the contribution of the longitudinal reinforcement. The second one is the uncracked transformed moment of inertia (I_{ucr}), which takes the contribution of the main reinforcement into account by transforming it to an equivalent concrete area according to the modular ratio of the two materials. The gross moment of inertia expression for all beams is given in (1) The uncracked moment of inertia expressions for the beams with and without compression reinforcement are given in (2) and (3):

$$I_g = \frac{bh^3}{12} \tag{1}$$

$$I_{ucr} = \frac{bh^3}{12} + bh\left(y' - \frac{h}{2}\right)^2 + \left(n_f - 1\right)A_{frp}\left(d - y'\right)^2 + \left(n-1\right)A_{st}\left(d - y'\right)^2 + \left(n-1\right)A_{cs}\left(d_{cc} - y'\right)^2 \tag{2}$$

$$I_{ucr} = \frac{bh^3}{12} + bh\left(y' - \frac{h}{2}\right)^2 + \left(n_f - 1\right)A_{frp}\left(d - y'\right)^2 + \left(n-1\right)A_{st}\left(d - y'\right)^2 \tag{3}$$

The terms b and h in these equations refer to the width (breadth) and height of the cross-section. Furthermore, the n and n_f ratii refer to the modular ratio of steel and FRP to concrete, respectively. The vertical distance of the neutral axis

to the compression face is shown with y'. A_{st}, A_{frp} and A_{cs} indicate the cross-sectional areas of the steel tension, FRP tension and compression reinforcement ratii, respectively. d_{cc} is the vertical distance of the centroid of the compression reinforcement to the compression face of the beam.

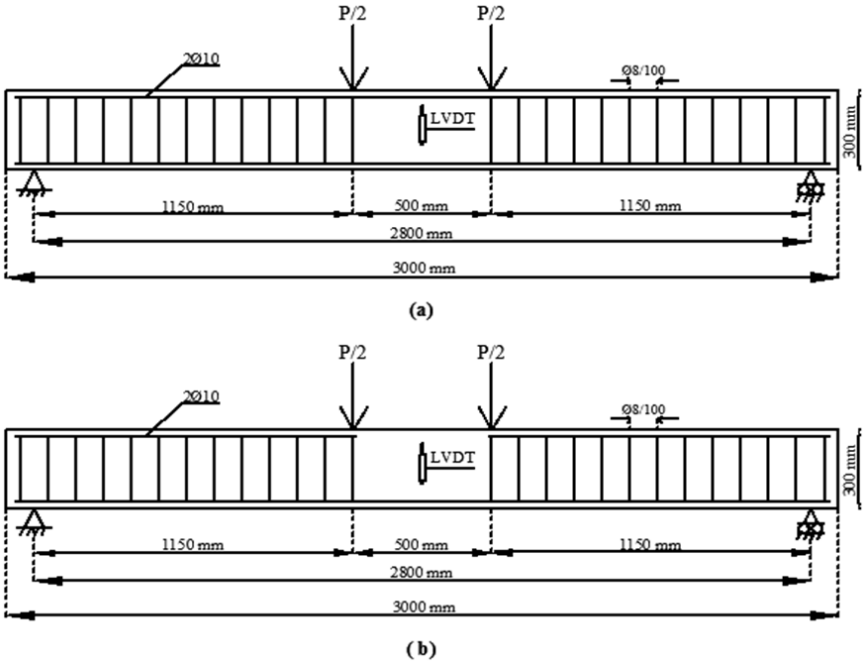

Fig. 1 Loading and support conditions and transverse reinforcement details of the beams cast in the (a) first batch (with compression reinforcement in the central region) and (b) in the second batch (without compression reinforcement in the central region)

B. Flexural Tensile Strength

In the cracking moment calculations, three different tensile strength values were utilized. The first one is the experimental value calculated from the prismatic beam tests under two-point loading (four-point bending) conducted for each concrete batch according ASTM C78 [10]. The second and third strength values for each batch were obtained from the empirical flexural tensile strength expressions of the two international concrete codes, i.e. Eurocode 2 [8] and ACI 318M [9]. For each flexural tensile strength expression, two cracking moment estimates were developed, one for the gross moment of inertia and the other for the uncracked transformed moment of inertia (Fig. 2). In this respect, the cracking moment values were determined according to the following equations:

$$M_{cr1} = \frac{I_{ucr}\ f_{ctf}}{y_t} \tag{4}$$

$$M_{cr2} = \frac{I_g\ f_{ctf}}{y_t} \tag{5}$$

M_{cr1} and M_{cr2} indicate the cracking moment values of the specimens calculated by using the uncracked transformed and gross moment of inertia expressions, respectively. y_t denoted the distance of the extreme tension fibers of the beam from neutral axis. The cracking load values of the beams corresponding to the uncracked transformed and gross moments of inertia (P_{cr1}, P_{cr2}) are to be calculated from the respective cracking moment values based on the loading and support conditions of the beam.

The flexural tensile strength of concrete according to Eurocode 2 [8] is calculated from (6) and the average direct tensile strength of concrete used in this equation can be determined from (7). The cracking moment values based on the tensile strength expression of Eurocode 2 [8] are calculated from (8), (9):

$$f_{ctm,fl} = \max\{(1.6 - h/1000) f_{ctm}\ ;\ f_{ctm}\} \tag{6}$$

$$f_{ctm} = 0.30 \times f_{ck}^{2/3} \le C50/60 \tag{7}$$

$$M_{cr1,EC2} = \frac{I_{ucr}\ f_{ctm,fl}}{y_t} \tag{8}$$

$$M_{cr2,EC2} = \frac{I_g\ f_{ctm,fl}}{y_t} \tag{9}$$

$M_{cr1,EC2}$ and $M_{cr2,EC2}$ refer to the cracking moments of the beams according to the Eurocode 2 [8] formulation based on the uncracked transformed and gross moments of inertia, respectively. Furthermore, $P_{cr1,EC2}$ and $P_{cr2,EC2}$ are the load values corresponding to the $M_{cr1,EC2}$ and $M_{cr2,EC2}$ cracking moments. Finally, the flexural tensile strength of concrete according to ACI 318 code [9] is calculated from (10), where

f'_c is in MPa.

TABLE I
PROPERTIES OF THE TESTED BEAMS

Specimen	Dimensions of cross section (mm)	Details of tensile reinforcement	Details of compression reinforcement	Cylinder Compressive Strength (MPa)	Modulus of Elasticity of FRP (GPa)	FRP Tensile Strength (MPa)	Failure mode
S5 Reference	200x300	5ϕ12 Steel	2ϕ10 Steel	31,28[a]	-	-	Under RC
S6 Reference	199.8x303.29	6ϕ12 Steel	-	30,49[b]	-	-	Under RC
S3 Reference	200.8x304.71	3ϕ12 Steel	-	30,49[b]	-	-	Under RC
B5 Reference	200x300	5ϕ8.68 BFRP	2ϕ10 Steel	31,28[a]	43	1034	Over RC
G5 Reference	200x300	5ϕ12.86 GFRP	2ϕ10 Steel	31,28[a]	35	449	Over RC
G6 Reference	200x307	6ϕ12.23 GFRP	-	30,49[b]	46	580	Over RC
G3 Reference	198.8x308.71	3ϕ12.23 GFRP	-	30,49[b]	46	580	Over RC
B2S3	200x300	2ϕ8.68 BFRP + 3ϕ12 Steel	2ϕ10 Steel	31,28[a]	43	1034	Over RC
B3S2	200x300	3ϕ8.68 BFRP + 2ϕ12 Steel	2ϕ10 Steel	31,28[a]	43	1034	Over RC
B4S1	200x300	4ϕ8.68 BFRP + 1ϕ12 Steel	2ϕ10 Steel	31,28[a]	43	1034	Over RC
G2S3	200x300	2ϕ12.86 GFRP + 3ϕ12 Steel	2ϕ10 Steel	31,28[a]	35	449	Over RC
G3S2	200x300	3ϕ12.86 GFRP + 2ϕ12 Steel	2ϕ10 Steel	31,28[a]	35	449	Over RC
G4S1	200x300	4ϕ12.86 GFRP + 1ϕ12 Steel	2ϕ10 Steel	31,28[a]	35	449	Over RC
G1S5	200.8x301.86	1ϕ12.23 GFRP + 5ϕ12 Steel	-	30,49[b]	46	580	Over RC
G2S4	199.8x301.14	2ϕ12.23 GFRP + 4ϕ12 Steel	-	30,49[b]	46	580	Over RC
G3S3	200.6x304.43	3ϕ12.23 GFRP + 3ϕ12 Steel	-	30,49[b]	46	580	Over RC
G4S2	198.6x304.57	4ϕ12.23 GFRP + 2ϕ12 Steel	-	30,49[b]	46	580	Over RC
G5S1	200.6x306	5ϕ12.23 GFRP + 1ϕ12 Steel	-	30,49[b]	46	580	Over RC
B1S2	199.8x308	1ϕ8.68 BFRP + 2ϕ12 Steel	-	30,49[b]	43	1034	Over RC
B1S4	200x300	1ϕ8.68 BFRP + 4ϕ12 Steel	2ϕ10 Steel	31,28[a]	43	1034	Under RC
G1S4	200x300	1ϕ12.86 GFRP + 4ϕ12 Steel	2ϕ10 Steel	31,28[a]	35	449	Under RC
B2S1	199.2x301.71	2ϕ8.68 BFRP + 1ϕ12 Steel	-	30,49[b]	43	1034	Under RC
G1S2	198.6x304.86	1ϕ12.23 GFRP + 2ϕ12 Steel	-	30,49[b]	46	580	Under RC
G2S1	202x301.57	2ϕ12.23 GFRP + 1ϕ12 Steel	-	30,49[b]	46	580	Under RC

a first bacth, b second batch of concrete.

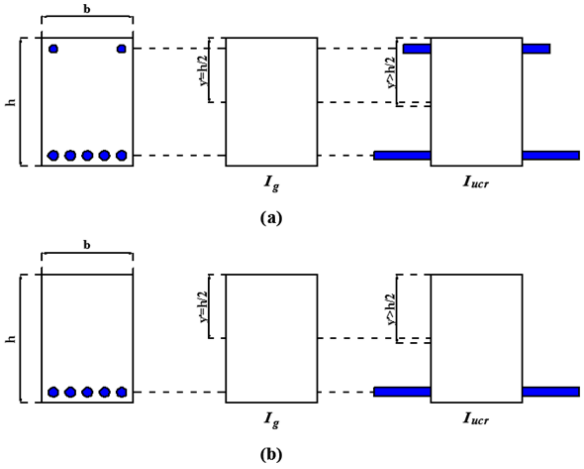

Fig. 2 The gross and uncracked moment of inertia calculations for the beam (a) with; (b) without compression reinforcement

Finally, the flexural tensile strength of concrete according to ACI 318M code [9] is calculated from (10), where f'_c is the specified compressive strength of concrete in MPa.

$$f_r = 0.623\sqrt{f'} \tag{10}$$

The cracking moment values of the beams according to the ACI 318M code [9] formulation and based on the two moment of inertia definitions can be obtained from:

$$M_{cr1,ACI} = \frac{I_{ucr}\ f_r}{y_t} \tag{11}$$

$$M_{cr2,ACI} = \frac{I_g\ f_r}{y_t} \tag{12}$$

The cracking load values corresponding to these two cracking moment definitions are denoted as $P_{cr1,ACI}$ and $P_{cr2,ACI.}$

IV. Comparison of the Experimental and Analytical Results

Tables II-V present the experimental cracking load values of the only steel-, only FRP-, hybrid over- and hybrid under-RC beam specimens, respectively, together with six different types of analytical estimates based on two different definitions of moment of inertia (gross, uncracked transformed) and three different definitions for modulus of rupture (prismatic test, Eurocode 2 and ACI 318M). Additionally, the mean and coefficient of variation (COV) values for each type of analytical estimate were also given in the table for the sake of comparison. As clearly seen from Table II, the experimental cracking load values of steel-reinforced specimens exceed the analytical values, significantly. The analytical estimates obtained by using the uncracked transformed moment of

inertia are in closer agreement with the experimental values as compared to the ones from the gross moment of inertia. The closest estimates were obtained when the uncracked transformed moment of inertia expression was used in combination with the modulus of rupture definition of Eurocode 2 with a mean value of 1.063 and a COV about %5. Since the modulus of elasticity of steel is high, ignoring the contribution of steel to the section, i.e. using the gross moment of inertia, results in considerable errors in analytical estimates. The differences between the cracking moment estimates according to the gross and uncracked transformed moment of inertia are higher in steel-reinforced beam group compared to the other groups due to the significant contribution of steel to the flexural response in the uncracked stage.

In beams with only FRP reinforcement (Table III), on the other hand, all of the estimated values are well above the experimental cracking moment values. In other words, none of the cracking moment expressions can provide close and conservative estimates in beams reinforced with only FRP bars. Among different analytical formulations, the use of the experimental modulus of rupture in combination with the gross moment of inertia yields to estimates in closest agreement with the experimental beam cracking loads with a mean of 0.743 and percent COV of about 16 % for the experimental-to-estimated load ratio. Among the two code expressions, the use of the ACI 318M [9] modulus of rupture in combination with the gross moment of inertia yielded to closer estimates as compared to the Eurocode 2 [8] strength expression. The differences between the estimates corresponding to the gross and uncracked transformed moment of inertia are really small due to the low modulus of elasticity value of FRP bars.

For over-reinforced beams with the simultaneous use of FRP and steel bars (Table IV), the closest analytical estimates were attained when using the uncracked transformed moment of inertia in combination with the experimental modulus of rupture (mean value of 0.982 and COV of 11%). The concept of over-reinforcement in hybrid beams corresponds to the beam behavior with concrete crushing preceding the FRP rupture, but following steel yielding. In both over- and under-reinforced hybrid beam groups, steel yielding took place long before concrete crushing and FRP rupture. The difference between over- and under-reinforcement stems from the order of concrete crushing and FRP rupture. Among completely empirical equations, the use of the ACI 318M [9] modulus of rupture together with the uncracked transformed moment of inertia yielded to closer estimates (mean value of 0.966 and COV of 11%).

In hybrid under-RC beams (Table V), on the other hand, the use of the ACI 318M [9] modulus of rupture in combination with the uncracked transformed moment of inertia yielded to the closest estimates (mean value of 1.028 and COV of 9%). These estimates are more accurate even compared to the ones from the experimental flexural tensile strength. The estimates for under-reinforced hybrid concrete beams can be seen to be generally conservative, while the ones for the over-reinforced beams generally remain on the non-conservative side.

V. Conclusions

The first cracking moments of steel-reinforced, FRP-reinforced and hybrid FRP-steel RC beams were estimated using different modulus of rupture and uncracked moment of inertia values in the present study. Hybrid beams in both under-reinforced and over-reinforced range of beam behavior were examined in the study. The results of 24 RC beam tests, conducted within the scope of a research project, were adopted in comparison. The most significant outcomes of the present investigation are as follows:

- Ignoring the contribution of the longitudinal reinforcement to the moment of inertia at the uncracked stage has little or no influence on the cracking moment estimates of FRP-RC beams as expected, while this assumption has deep influence on the cracking moment estimates of steel-RC beams. The difference between the FRP- and steel-RC beams stems from the fact that the moment of inertia of steel is much larger than the respective values of FRP bars. Accordingly, the uncracked transformed moment of inertia should be used in the estimation of cracking moments of steel-RC beams, while both the gross and uncracked transformed moments of inertia can be used with little difference in FRP-RC beams.
- In beams with hybrid FRP-steel reinforcement, closest analytical cracking moment estimates are obtained by using the modulus of rupture expression of the ACI 318M [9] code and the uncracked transformed moment of inertia. The analytical cracking moment estimates were observed to remain on the conservative side in under-reinforced hybrid beams, while remaining on the non-conservative side in over-reinforced ones.
- The initial cracking moment values of FRP-RC beams cannot be predicted accurately by using the modulus of rupture and moment of inertia expressions adopted in the present study. This is most probably caused by the material imperfections and nonlinearities related to the FRP bars, i.e. the misalignment of the fibers in the composite, the relative slip between the fibers and composite matrix and the slip of the bar in concrete up to the formation of full FRP-concrete bond strength.

The analytical estimates were observed to be well below the experimental cracking moment values in FRP-RC beams.

- The Eurocode 2 [8] modulus of rupture expression produced the closest first cracking moment estimates in steel-RC beams, particularly when used in combination with the uncracked transformed moment of inertia.

TABLE II
FIRST CRACKING LOAD PREDICTIONS FOR ONLY STEEL RC BEAMS

Specimen	$P_{cr,exp}$ (kN)	P_{cr1} (kN)	P_{cr2} (kN)	$P_{cr,exp}/P_{cr1}$	$P_{cr,exp}/P_{cr2}$	$P_{cr1,EC2}$ (kN)	$P_{cr2,EC2}$ (kN)	$P_{cr,exp}/P_{cr1,EC2}$	$P_{cr,exp}/P_{cr2,EC2}$	$P_{cr1,ACI}$ (kN)	$P_{cr2,ACI}$ (kN)	$P_{cr,exp}/P_{cr1,ACI}$	$P_{cr,exp}/P_{cr2,ACI}$
S5 Reference	25.70	22.29	18.52	1.15	1.39	24.30	20.19	1.06	1.27	21.85	18.16	1.18	1.42
S6 Reference	27.74	21.05	17.3	1.32	1.6	24.68	20.28	1.12	1.37	22.28	18.31	1.24	1.52
S3 Reference	23.13	19.45	17.55	1.19	1.32	22.8	20.57	1.01	1.12	20.59	18.57	1.12	1.25
Standard Deviation				0.089	0.146			0.055	0.126			0.060	0.136
Mean				1.220	1.437			1.063	1.254			1.179	1.395
COV (%)				7.285	10.143			5.192	10.048			5.094	9.757

TABLE III
FIRST CRACKING LOAD PREDICTIONS FOR ONLY FRP RC BEAMS

Specimen	$P_{cr,exp}$ (kN)	P_{cr1} (kN)	P_{cr2} (kN)	$P_{cr,exp}/P_{cr1}$	$P_{cr,exp}/P_{cr2}$	$P_{cr1,EC2}$ (kN)	$P_{cr2,EC2}$ (kN)	$P_{cr,exp}/P_{cr1,EC2}$	$P_{cr,exp}/P_{cr2,EC2}$	$P_{cr1,ACI}$ (kN)	$P_{cr2,ACI}$ (kN)	$P_{cr,exp}/P_{cr1,ACI}$	$P_{cr,exp}/P_{cr2,ACI}$
B5 Reference	14.53	19.08	18.52	0.76	0.78	20.8	20.19	0.7	0.72	18.71	18.16	0.78	0.8
G5 Reference	11.08	19.11	18.52	0.58	0.6	20.83	20.19	0.53	0.55	18.73	18.16	0.59	0.61
G6 Reference	12.45	18.2	17.74	0.68	0.7	21.34	20.8	0.58	0.6	19.27	18.78	0.65	0.66
G3 Reference	15.93	18.06	17.83	0.88	0.89	21.18	20.9	0.75	0.76	19.12	18.87	0.83	0.84
Standard Deviation				0.127	0.123			0.102	0.099			0.111	0.110
Mean				0.725	0.743			0.640	0.658			0.713	0.728
COV (%)				17.501	16.545			15.985	15.024			15.645	15.115

TABLE IV
FIRST CRACKING LOAD PREDICTIONS FOR HYBRID OVER-RC BEAMS

Specimen	$P_{cr,exp}$ (kN)	P_{cr1} (kN)	P_{cr2} (kN)	$P_{cr,exp}/P_{cr1}$	$P_{cr,exp}/P_{cr2}$	$P_{cr1,EC2}$ (kN)	$P_{cr2,EC2}$ (kN)	$P_{cr,exp}/P_{cr1,EC2}$	$P_{cr,exp}/P_{cr2,EC2}$	$P_{cr1,ACI}$ (kN)	$P_{cr2,ACI}$ (kN)	$P_{cr,exp}/P_{cr1,ACI}$	$P_{cr,exp}/P_{cr2,ACI}$
B2S3	23	21.02	18.52	1.09	1.24	22.91	20.19	1	1.14	20.6	18.16	1.12	1.27
B3S2	20.09	20.37	18.52	0.99	1.08	22.21	20.19	0.9	1	19.97	18.16	1.01	1.11
B4S1	18.02	19.73	18.52	0.91	0.97	21.51	20.19	0.84	0.89	19.34	18.16	0.93	0.99
G2S3	20	21.03	18.52	0.95	1.08	22.92	20.19	0.87	0.99	20.61	18.16	0.97	1.1
G3S2	17.62	20.39	18.52	0.86	0.95	22.23	20.19	0.79	0.87	19.99	18.16	0.88	0.97
G4S1	18.32	19.75	18.52	0.93	0.99	21.53	20.19	0.85	0.91	19.36	18.16	0.95	1.01
G1S5	23.09	20.41	17.22	1.13	1.34	23.93	20.19	0.97	1.14	21.6	18.23	1.07	1.27
G2S4	22.01	19.69	17.05	1.12	1.29	23.08	19.99	0.95	1.1	20.84	18.05	1.06	1.22
G3S3	18.85	19.62	17.5	0.96	1.08	23	20.51	0.82	0.92	20.77	18.52	0.91	1.02
G4S2	19.14	18.91	17.34	1.01	1.1	22.17	20.33	0.86	0.94	20.02	18.35	0.96	1.04
G5S1	14.17	18.7	17.68	0.76	0.8	21.92	20.72	0.65	0.68	19.79	18.71	0.72	0.76
B1S2	20.55	19.16	17.84	1.07	1.15	22.46	20.91	0.91	0.98	20.28	18.88	1.01	1.09
Standard Deviation				0.111	0.153			0.093	0.129			0.104	0.143
Mean				0.982	1.089			0.868	0.963			0.966	1.071
COV (%)				11.275	14.036			10.680	13.392			10.809	13.353

TABLE V
FIRST CRACKING LOAD PREDICTIONS FOR HYBRID UNDER-RC BEAMS

Specimen	$P_{cr,exp}$ (kN)	P_{cr1} (kN)	P_{cr2} (kN)	$P_{cr,exp}/P_{cr1}$	$P_{cr,exp}/P_{cr2}$	$P_{cr1,EC2}$ (kN)	$P_{cr2,EC2}$ (kN)	$P_{cr,exp}/P_{cr1,EC2}$	$P_{cr,exp}/P_{cr2,EC2}$	$P_{cr1,ACI}$ (kN)	$P_{cr2,ACI}$ (kN)	$P_{cr,exp}/P_{cr1,ACI}$	$P_{cr,exp}/P_{cr2,ACI}$
B1S4	24.39	21.66	18.52	1.13	1.32	23.61	20.19	1.03	1.21	21.23	18.16	1.15	1.34
G1S4	22.89	21.66	18.52	1.06	1.24	23.61	20.19	0.97	1.13	21.23	18.16	1.08	1.26
B2S1	18.84	17.76	17.07	1.06	1.1	20.82	20.01	0.9	0.94	18.8	18.06	1	1.04
G1S2	19.83	18.72	17.37	1.06	1.14	21.94	20.37	0.9	0.97	19.81	18.39	1	1.08
G2S1	17.32	18.07	17.29	0.96	1	21.18	20.27	0.82	0.85	19.12	18.3	0.91	0.95
Standard Deviation				0.061	0.124			0.080	0.147			0.091	0.161
Mean				1.054	1.160			0.924	1.020			1.028	1.134
COV (%)				5.756	10.698			8.611	14.375			8.846	14.214

REFERENCES

[1] M. A. Aiello and L. Ombres, "Structural performances of concrete beams with hybrid (fiber-reinforced polymer-steel) reinforcements," Journal of Composites for Construction, vol. 6, no. 2, pp. 133-140, May 2002.

[2] H. Y. Leung and R. V. Balendran, "Flexural behaviour of concrete beams internally reinforced with GFRP rods and steel rebars," Structural Survey, vol. 21, no. 4, pp. 146-157, 2003.

[3] W. Qu, X. Zhang and H. Huang, "Flexural behavior of concrete beams

reinforced with hybrid (GFRP and steel) bars," Journal of Composites for Construction, vol. 13, no. 5, pp. 350-359, Sep. 2009.
[4] D. Lau and H. J. Pam, "Experimental study of hybrid FRP reinforced concrete beams," Engineering Structures, vol. 32, pp. 3857-3865, 2010.
[5] M. A. Safan, "Flexural behavior and design of steel-GFRP reinforced concrete beams," ACI Materials Journal, vol. 110, no. 6, pp.-677-685, Nov.-Dec. 2013.
[6] L. Yinghao and Y. Yong, "Arrangement of hybrid rebars on flexural behavior of HSC beams," Composites: Part B, vol. 45, pp. 22-31, 2013.
[7] M. Yaz, "The Effect of GFRP Bars on Flexural Behaviour in Reinforced Concrete Beams," Graduate School of Natural and Applied Sciences, Department of Civil Engineering, M. Sc. Thesis, Kirikkale University, Aug. 2014.
[8] Comité Européen de Normalisation (CEN), "prEN 1992-1-1:2004 (Eurocode 2): Design of Concrete Structures - Part 1-1: General Rules and Rules for Buildings," European Committee for Standardization (CEN), Brussels, Belgium, 2004.
[9] ACI Committee 318M, "Building Code Requirements for Structural Concrete (ACI 318M-11) and Commentary," American Concrete Institute, Farmington Hills, Michigan, U.S.A., 2011.
[10] ASTM C78 / C78M-18, "Standard Test Method for Flexural Strength of Concrete (Using Simple Beam with Third-Point Loading)," ASTM International, West Conshohocken, PA, 2018.